An Optimized Index of Human Cardiovascular Adaptation to Simulated Weightlessness

Mao Wang,* Laurence Hassebrook, *Member, IEEE,* Joyce Evans, Tomy Varghese, *Member, IEEE,* and Charles Knapp

Abstract— **Prolonged exposure to weightlessness is known to produce a variety of cardiovascular changes, some of which may influence the astronaut's performance during a mission. In order to find a reliable indicator of cardiovascular adaptation to weightlessness, we analyzed data from nine male subjects after a 24-hour period of normal activity and after a period of simulated weightlessness produced by two hours in a launch position followed by 20 hours of 6° head-down tilt plus pharmacologically induced diuresis (furosemide). Heart rate, arterial pressure, thoracic fluid index, and radial flow were analyzed. Autoregressive spectral estimation and decomposition were used to obtain the spectral components of each variable from the subjects in the supine position during pre- and post-simulated weightlessness. We found a significant decrease in heart rate power and an increase in thoracic fluid index power in the high frequency region (0.2–0.45 Hz) and significant increases in radial flow and arterial pressure powers in the low frequency region (<0.2 Hz) in response to simulated weightlessness. However, due to the variability among subjects, any single variable appeared limited as a dependable index of cardiovascular adaptation to weightlessness. The backward elimination algorithm was then used to select the best discriminatory features from these spectral components. Fisher's linear discriminant and Bayes' quadratic discriminant were used to combine the selected features to obtain an optimal index of adaptation to simulated weightlessness. Results showed that both techniques provided improved discriminant performance over any single variable and thus have the potential for use as an index to track adaptation and prescribe countermeasures to the effects of weightlessness.**

I. Introduction

EXPOSURE to microgravity or weightlessness is known to produce a variety of cardiovascular (CV) changes or adaptations [1]–[13]. Depending on the length of the exposure, these changes may be relatively subtle or may result in orthostatic hypotension which could influence or significantly compromise the astronaut's performance during a mission.

The majority of studies that examined CV changes in response to actual or simulated weightlessness concentrated on the static levels of cardiovascular variables, such as mean heart rate and blood pressure. The monitoring of mean values alone is not the only way of assessing weightlessness-induced adaptation in cardiovascular regulation. Quantification of the dynamic properties of CV variables through spectral analysis has also been shown to provide an analytical tool to assess relative contributions from neural pathways involved in cardiovascular regulation [14]–[19].

To assess the potential of using the dynamic properties of CV variables as an index to track weightlessness-induced changes in CV regulation, we employed spectral analysis and discrimination techniques to data acquired noninvasively and continuously from human subjects after 24 hours of normal activities and after 22 hours of simulated weightlessness (SW). A schematic diagram for obtaining this index is depicted in Fig. 1. After acquiring data from subjects after 24 hours of normal activity, we exposed these subjects to a simulated weightlessness protocol consisting of two hours in the launch position followed by 20 hours of 6° head-down tilt (HDT) [4], [5], [8]–[12] plus pharmacologically induced diuresis (furosemide) to accelerate volume depletion. Applying discrimination techniques to spectral contents of CV variables in this study allowed us to detect consistent changes in cardiovascular parameters which appear to indicate adaptation to simulated weightlessness.

Our objective is to assess the ability of *spectral* features, acquired from noninvasively and continuously monitored CV variables, to reliably predict cardiovascular adaptation in CV regulation induced by simulated weightlessness. In the present study, we demonstrated that individual CV variables varied considerably across subjects. However, when combined in the form of a Fisher's linear discriminant or Bayes' quadratic discriminant, the variance was considerably decreased and the discrimination performance was improved. In future research, these measures can be tested as reliable indexes of an astronaut's adaptation to spaceflight in microgravity.

II. Simulated Weightlessness

Ten healthy male volunteers [25.8 ± 1.4 yrs, 179.6 ± 1.4 cm, 76.5 ± 2 kg (data are represented as mean ±SEM)] participated in the experiment (a similar study in female subjects in pre SW state is currently being conducted). All but two of the subjects in this study regularly engaged in some form of aerobic exercise ranging from 3–20 miles/week of running, jogging or walking (average 8.1 ± 2.6 miles/week). The volunteers were screened prior to the experiment to verify that no previous medical problem existed. On the day of the experiment, impedance leads were attached for measurement of the electrocardiogram, thoracic fluid index (TFI), rate of change of thoracic impedance and beat-by-

Manuscript received July 2, 1993; revised December 6, 1995. This work was supported by NASA under Grant 9-298 and the Clinical Research Center under Grant M01-RR-2602. *Asterisk indicates corresponding author.*

*M. Wang is with the Motorola Cellular Infrastructure Group, Arlington Heights, IL 60004 USA (e-mail: wangmm@cig.mot.com).

L. Hassebrook, J. Evans, T. Varghese, and C. Knapp are with the Center for Biomedical Engineering, and Department of Electrical Engineering, University of Kentucky, Lexington, KY 40506-0070 USA.

Publisher Item Identifier S 0018-9294(96)03186-2.

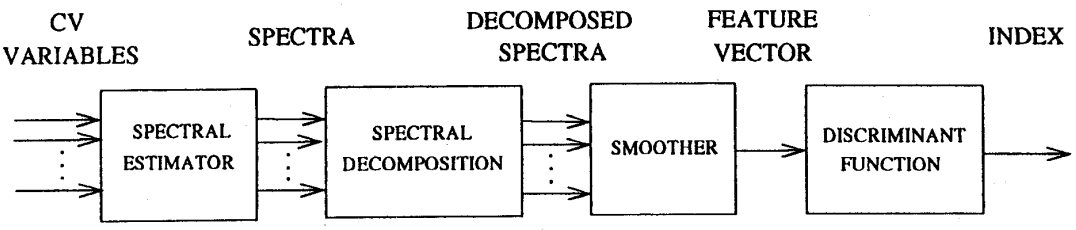

Fig. 1. Schematic diagram for the implementation of an index of adaptation to weightlessness.

beat estimates of left-ventricular end-diastolic volume (EDV), stroke volume (SV), and cardiac output (CO) (Bomed, Cardiodynamic Monitor, BoMed Inc., Irvine, CA). Continuous measurements of peripheral arterial pressure (AP) [(Finapres, Ohmeda, Englewood, CO), calibrated with an upper arm cuff (Sentry, NBS Medical, Cosa Mesta, CA)], and ascending aortic blood flow velocity using continuous wave doppler (Exerdop, Quinton Instruments, Seattle, WA) and radial flow (RF) (Parks, Model 909 Directional Doppler, Parks Medical, Beaverton, OR) were also made. Heart rate (HR) was calculated from R–R intervals in the ECG. After a 30-min supine control period, the subjects underwent a series of step and sinusoidal lower body negative pressure (LBNP) tests to assess frequency response characteristics of these subjects [20]–[22]. After an ambulatory period, the subject was reinstrumented and placed in the launch position for two hours followed by 20 hours of 6° HDT. In order to simulate the fluid loss of space flight, 40 mg of the diuretic furosemide was administered by mouth after two hours of 6° HDT. (Because the half life of furosemide is relatively short, 92 ± 7 minutes [23], the direct effects were unlikely to influence hemodynamic data 18 hours after administration of furosemide.) At the end of the 20 hours of HDT, the subjects were returned to supine for 30 min. Pre- and post-SW data from nine subjects during the 30 min supine rest periods were used to develop the adaptation index; the other subject was used to test the index.

Table I lists mean values of major hemodynamic parameters in these 10 subjects before and after SW. There was a negative fluid balance (fluid in–fluid out) of 497 ± 167 ml ($p < 0.01$) which was reflected in significantly decreased stroke volume and central venous pressure. The regulatory response to the change in fluid balance included an increase in vascular resistance mediated by increases in the vasoactive hormones renin and norepinephrine. The net result, with respect to mean values, was that blood pressure did not reflect the decrease in stroke volume but was actually slightly increased. The blood pressure regulatory capability of these subjects in response to blood pooling induced by graded levels of LBNP was tested before and after SW [20]. We determined that, after SW, the maintenance of blood pressure during LBNP stress required significantly higher levels of mean HR and TPR. This loss of orthostatic reserve is one symptom of the phenomenon labeled orthostatic intolerance or cardiovascular deconditioning which develops with exposure to real or simulated weightlessness [1]–[6]. In the following sections the neural components of the regulatory response to SW will be explored using spectral analysis and discrimination techniques to obtain an optimized index of sympathetic and parasympathetic autonomic balance.

TABLE I
MEAN VALUES OF HEMODYNAMIC PARAMETERS BEFORE AND AFTER SW TAKEN FROM 10 SUBJECTS

Variable	Pre SW	Post SW
HR (bpm)	67.1±4.0	68.5±4.6
AP (mmHg)	89.0±2.2	90.6±2.1
CVP (mmHg)	3.38±0.58	1.55±0.76*
SV (ml)	86.0±12.3	74.8±15.3*
TPR (mmHg/(L/min))	15.4±3.3	18.7±3.3
Plasma renin (ng/ml/hr)	1.81±0.22	3.6±0.58*
Epinephrine (pg/ml)	25.8±4.2	29.7±5.1
Norepinephrine (pg/ml)	79.9±12.3	100.4±13.5*

* Significantly ($p < 0.05$) different from pre SW.
TPR = Total peripheral resistance.

III. SPECTRAL ANALYSIS

The choice of CV variables to include in this index was based on both standard spectral measurements and measurements from variables that could provide insight into the fluid volume shifts associated with SW. The standard spectral indexes, HR and AP, have been explored extensively for their ability to provide quantitative information about changes in the balance between sympathetic and parasympathetic components. Previous studies in our laboratory [20]–[22] have shown that SW evoked changes in HR and AP spectral power that were statistically significant. The decision to include variables that reflected the fluid volume shifts associated with SW was based on the consistent findings that both true and simulated weightlessness have been shown to translocate vascular volume from peripheral to thoracic regions [1], [2], [4], [11], [13]. Our indices of thoracic fluid index and peripheral flow were therefore used as indicators of the neurally mediated responses to this translocation of fluid.

HR, AP, TFI, and RF were digitized at 500 Hz using DATAQ and analyzed on an IBM RISC/6000. The data for each variable consisted of ~30 min during supine control before and after SW.

Data were low-pass filtered at 0.7 Hz and divided into 2.5-min-long segments that partially overlapped. Autoregressive (AR) spectral estimation techniques (Burg's algorithm [24])

TABLE II
BINNING FREQUENCIES

Variable	Frequency Range (Hz)	
	LF	HF
HR	0.003-0.10	0.20-0.45
TFI	0.003-0.10	0.10-0.45
RF	0.003-0.20	0.20-0.45
AP	0.003-0.05	0.20-0.45

were used to estimate the spectrum (0.003–0.5 Hz) of each 2.5-min data segment. The order of the AR spectrum was determined according to Akaike's final prediction error (FPE) criterion [25] and tests for whiteness [26] of the prediction error. The order ranged from 30–40. To reduce the effect of very low frequency trends on spectral estimation, each data segment was detrended using quadratic polynomial fitting prior to spectral estimation. The spectrum was then decomposed into low-frequency (LF) and high-frequency (HF) bins. HF spectral power has been reported to be indicative of parasympathetic influence on the cardiovascular regulatory system and LF power has been shown to be influenced by both parasympathetic and sympathetic branches of the autonomic nervous system [14]–[19]. The LF and HF bin widths for each variable were chosen to maximize the difference in spectral power in the bin between pre SW (G_1) and post SW (G_0). More specifically, for each variable, the highest frequency contained in the LF bin and the lowest frequency contained in the HF bin were determined so that the difference between the means of spectral power in that bin for G_0 and G_1 was maximum and the variance minimum while the lowest frequency of LF and highest frequency of HF were fixed at 0.003 and 0.4 Hz, respectively. That is, we defined the frequency range of LF and HF such that the distance between two sample class means relative to the dispersion within the classes, or the Mahalanobis distance

$$d^2(f) = \frac{|m_1(f) - m_0(f)|^2}{s_1^2(f) + s_0^2(f)} \tag{1}$$

was maximum, where f is the width of LF or HF in Hz, m_i and s_i^2 are the mean and variance of spectral power in LF or HF for G_i ($i = 0, 1$). The resultant binning frequencies for the variables are listed in Table II.

The power in LF and HF was computed by spectral decomposition. It can be shown that an AR spectrum

$$S(z) = \frac{P_M}{\left|1 + \sum_{i=1}^{M} a_i^{(M)} z^{-i}\right|^2} \tag{2}$$

can be decomposed into

$$S(z) = \sum_{j=1}^{M/2} \left[\frac{\alpha_j}{z - z_j} + \frac{-\left(\frac{1}{z_j^*}\right)^2 \alpha_j^*}{z - \frac{1}{z_j^*}} + \frac{\alpha_j^*}{z - z_j^*} + \frac{-\left(\frac{1}{z_j}\right)^2 \alpha_j}{z - \frac{1}{z_j}} \right] \tag{3}$$

where M (assume even) is the order of the AR model, z_j is the jth pole of $S(z)$, and α_j is the residual of $S(z)$ at z_j. The term in the bracket can be considered as the power attributable to pole z_j and its conjugate. The power in LF or HF can be computed by summation of the power related to the poles in LF or HF. An example of decomposed spectra is depicted in Fig. 2.

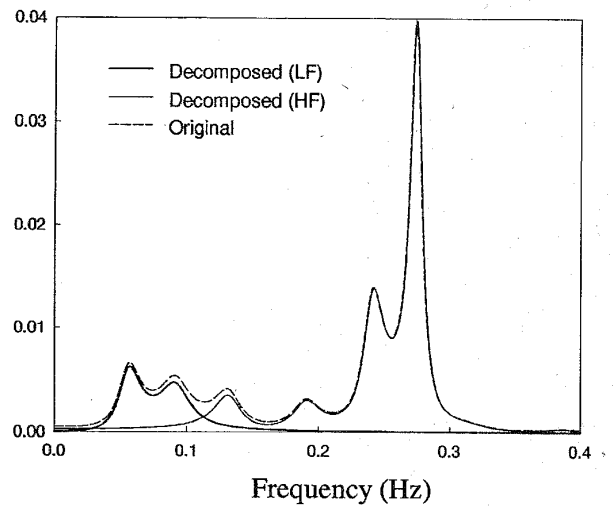

Fig. 2. A TFI spectrum decomposed into LF and HF bins using AR spectral decomposition.

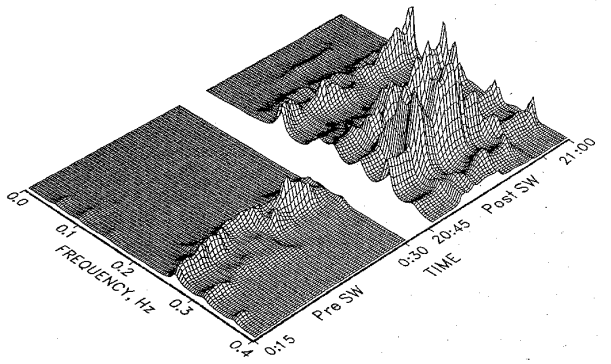

Fig. 3. TFI spectra across time before SW (15 min) and after SW (15 min) in one subject.

Fig. 3 presents TFI spectra across time for the second 15 min of the 30-min supine rest periods before and after SW in one subject, which shows changes in spectra between states as well as stability of spectra across time for each state. Single spectra taken near the end of 30-min supine rest, both before and after SW for each variable in one subject, are shown in Fig. 4. For the group of nine subjects, spectral differences in HR, TFI, RF, and AP were statistically significant after SW

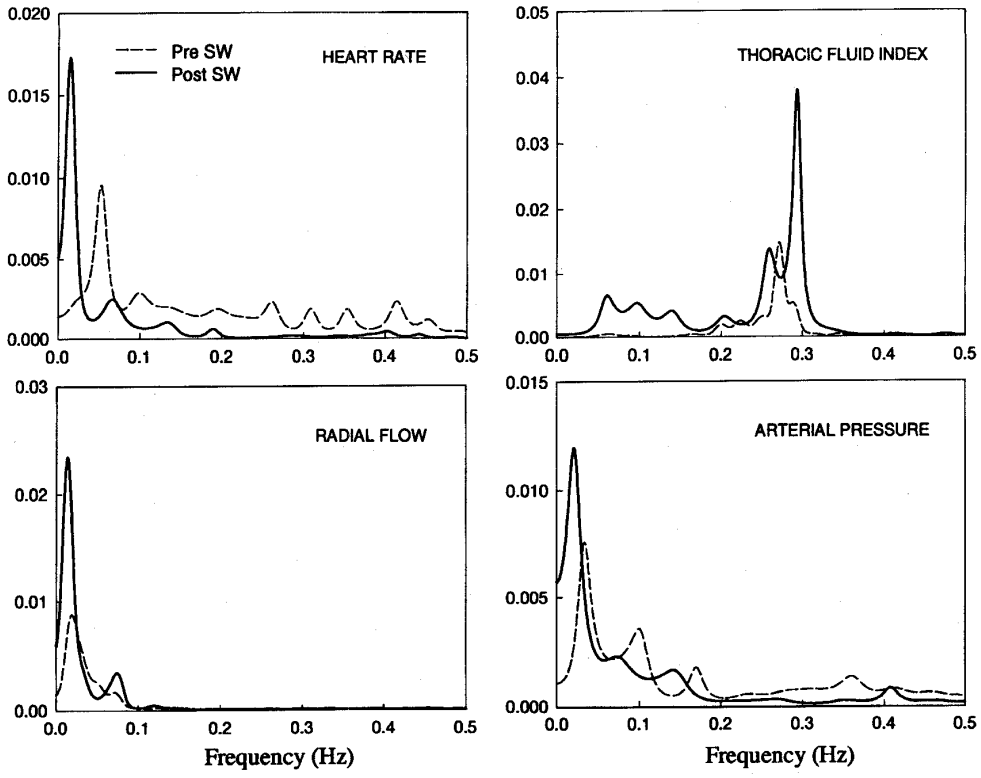

Fig. 4. Single spectra of HR, TFI, RF, and AP for one subject before and after SW.

(Fig. 5). The HF power of HR was significantly reduced after SW, while the HF power of TFI and LF power of RF and AP were significantly increased (Wilcoxon matched-pair signed-rank test [27], $p < 0.05$). The increase in overall total power of TFI in combination with the broadening of TFI spectra indicated that, after SW, breathing frequency was more varied and the depth of breathing was increased. The HR, AP, and RF results indicated a shift in autonomic balance toward reduced parasympathetic (decreased HF, HR power) and increased sympathetic (increased LF, AP, and RF powers) components of CV regulation after SW.

IV. Discriminant Analysis

The spectral components of the CV variables described in Section III were explored in order to obtain a reliable index of adaptation in CV regulation produced by our model of simulated weightlessness. As shown, some spectral components of some CV variables appear promising as features for discrimination of cardiovascular adaptation. However, these individual features exhibited considerable variability across subjects. To obtain an index with improved discriminatory performance, Fisher's linear discriminant function [28] was used to combine the features into an optimal feature, an index of adaptation to weightlessness, defined as a linear function of the feature vector $\underline{\boldsymbol{x}}$

$$l(\underline{\boldsymbol{x}}) = \underline{\boldsymbol{w}}^t \underline{\boldsymbol{x}} \tag{4}$$

where $\underline{\boldsymbol{w}}$, a feature weighting vector, maximizes the Rayleigh quotient

$$\Re(\underline{\boldsymbol{w}}) = \frac{\underline{\boldsymbol{w}}^t \boldsymbol{S}_B \underline{\boldsymbol{w}}}{\underline{\boldsymbol{w}}^t \boldsymbol{S}_W \underline{\boldsymbol{w}}}. \tag{5}$$

$\boldsymbol{S}_W$ is the within-class scatter matrix which is a pooled covariance matrix of the sample covariance matrices of the two classes G_0 and G_1

$$\boldsymbol{S}_W = \boldsymbol{S}_0 + \boldsymbol{S}_1 \tag{6}$$

and $\boldsymbol{S}_B$ is the between-class scatter matrix

$$\boldsymbol{S}_B = (\underline{\boldsymbol{m}}_1 - \underline{\boldsymbol{m}}_0)(\underline{\boldsymbol{m}}_1 - \underline{\boldsymbol{m}}_0)^t \tag{7}$$

where

$$\boldsymbol{S}_i = \sum_{\underline{\boldsymbol{x}} \in G_i} (\underline{\boldsymbol{x}}_i - \underline{\boldsymbol{m}}_i)(\underline{\boldsymbol{x}}_i - \underline{\boldsymbol{m}}_i)^t, \quad i = 0, 1 \tag{8}$$

and $\underline{\boldsymbol{m}}_i$ is the sample mean of G_i. It is easy to show [28] that a vector $\underline{\boldsymbol{w}}$ that maximizes $\Re(\underline{\boldsymbol{w}})$ is

$$\underline{\boldsymbol{w}} = \frac{\boldsymbol{S}_W^{-1}(\underline{\boldsymbol{m}}_1 - \underline{\boldsymbol{m}}_0)}{||\boldsymbol{S}_W^{-1}(\underline{\boldsymbol{m}}_1 - \underline{\boldsymbol{m}}_0)||}. \tag{9}$$

To examine the discriminatory properties of individual CV variables, the discriminant function was first applied to each variable. The feature vector was composed of the LF and HF power of that variable, such that

$$\underline{\boldsymbol{x}} = [x_{\mathrm{LF}} \quad x_{\mathrm{HF}}]^t. \tag{10}$$

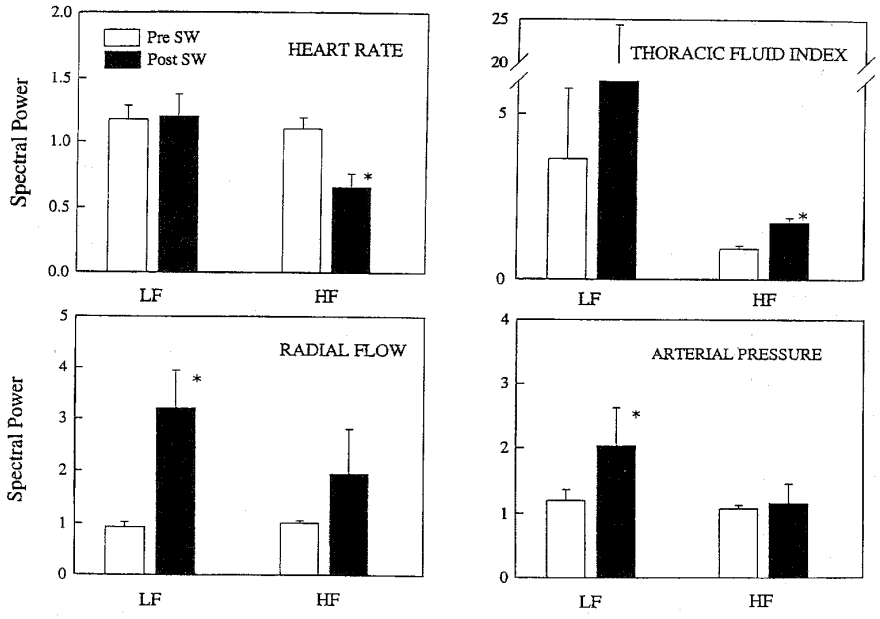

Fig. 5. LF and HF spectral powers of HR, TFI, RF, and AP averaged for nine subjects pre- and post-SW.

Different subjects have large differences in the spectral power of each variable which will introduce large variances. To reduce the variance introduced by each subject, the LF and HF power was normalized to each subjects's baseline (pre SW) spectral power

$$\underline{y} = \boldsymbol{A}^{-1}\underline{x} \tag{11}$$

where $\boldsymbol{A}$ is the normalization matrix

$$\boldsymbol{A} = \text{diag}\,[x^B_{\text{LF}} \quad x^B_{\text{HF}}]. \tag{12}$$

The elements x^B_{LF} and x^B_{HF} are the baseline LF and HF power, respectively, which are obtained from each subject prior to simulated weightlessness. In addition, when several CV variables are combined into a pattern vector, the original variables have physical units which are completely unconnected and may differ considerably in magnitude. Therefore, the round-off errors in the covariance matrices may be serious. This problem was reduced after normalization. Normalization also allows us to eliminate the absolute value from variables so that the weighting coefficient of a variable in $\underline{w}$ indicates the relative importance of discriminant information that the variable contains.

Fig. 6 shows the Fisher's discriminant applied separately to the HR, TFI, RF, and AP spectra (Fig. 4) for each of the nine subjects. If we treat these discriminant values as adaptation measures, we see that for each variable the discriminant of most subjects decreased after SW. However, there was a large deviation across subjects. Some subjects showed large adaptation in some variables and small or even opposite adaptation in the others.

To obtain a better index, we combined the best features from all possible CV variables into one feature vector. Inclusion of all spectral features may lead to unstable estimates of the feature weighting vector (or the discriminant function coefficients) if these features contain redundant information. Also, any feature which does not contribute to the index's predictive ability should be excluded since the more features included, the greater the costs of data collection and computation. The best features to include therefore, had to be determined. A *backward elimination* algorithm [29] was used to select a subset of important features from the complete set. The procedure starts with the complete set and then deletes one feature variable at a time until some stopping criterion is satisfied. The feature to be deleted is the one that decreases D^2 the least, where D^2 is the Mahalanobis distance

$$D^2 = (\underline{m}_1 - \underline{m}_2)^t S_W^{-1}(\underline{m}_1 - \underline{m}_2). \tag{13}$$

The Rao F statistic [30] was used as the stopping criterion to test the significance of a variable's contribution to the discrimination. The elimination procedure is shown in Table III. At stage 1, the LF component of TFI was selected for removal. At stage 2, the HF component of AP was removed. At stage 3, the LF component of HR was removed. At stage 4, the LF component of AP was removed, and at stage 5, the HF component of RF was removed. Elimination was then stopped since all the remaining features were significant at the 0.1 level ($F > 3.39$). The selected feature vector is, thereby

$$\underline{y} = [y_{\text{HR,HF}} \quad y_{\text{TFI,HF}} \quad y_{\text{RF,LF}}]^t. \tag{14}$$

A sample space spanned by HR (HF), TFI (HF), and RF (LF) is shown in Fig. 7, from which we can see that these two classes are separable. The feature weighting vector estimated from the training data set (taken from nine subjects near the beginning of the both pre- and post-SW supine rest periods) is $\underline{w} = [0.58 \ -0.78 \ -0.24]^t$. The corresponding Fisher's linear

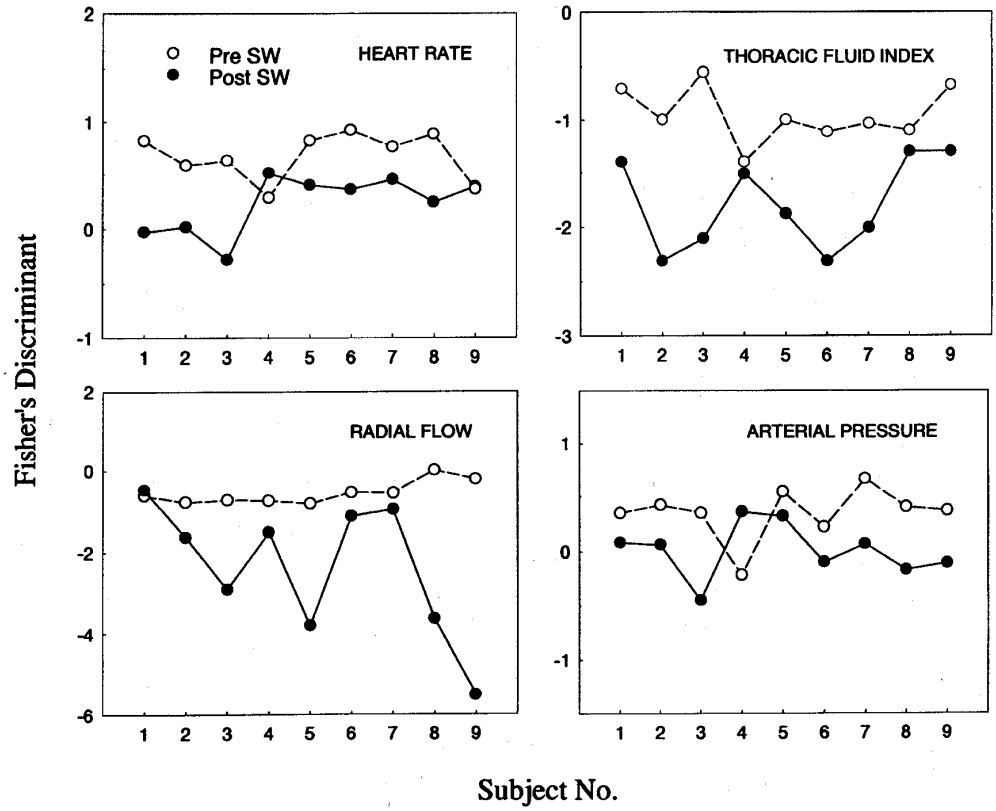

Fig. 6. Fisher's linear discriminants of HR, TFI, RF, and AP for nine subjects before and after SW.

TABLE III
FEATURE SELECTION USING BACKWARD ELIMINATION

Stage	1								2						
Variable Deleted	HR (LF)	HR (HF)	**TFI (LF)**	TFI (HF)	RF (LF)	RF (HF)	AP (LF)	AP (HF)	HR (LF)	HR (HF)	TFI (HF)	RF (LF)	RF (HF)	AP (LF)	**AP (HF)**
D^2	11.3	7.2	**12.6**	4.6	6.2	8.9	11.6	12.2	11.2	7.1	4.6	5.6	8.9	11.6	**12.2**
F	0.8	4.5	**0.1**	8.6	5.8	2.6	0.6	0.2	0.9	5.1	9.5	7.4	2.9	0.6	**0.2**

Stage	3						4					5				6		
Variable Deleted	**HR (LF)**	HR (HF)	TFI (LF)	RF (LF)	RF (HF)	AP (LF)	HR (HF)	TFI (HF)	RF (LF)	RF (HF)	**AP (LF)**	HF (HF)	TFI (HF)	RF (LF)	**RF (HF)**	HR (HF)	TFI (HF)	RF (LF)
D^2	**11.2**	7.0	4.0	5.6	8.5	10.9	5.7	4.3	4.2	7.4	**10.0**	5.6	3.8	3.2	**7.4**	4.5	1.2	2.6
F	**0.7**	5.3	10.0	7.7	3.4	1.0	6.6	10.2	10.6	3.6	**1.0**	6.1	10.7	12.6	**3.1**	4.8	17.5	10.7

discriminant function is

$$l(\underline{\boldsymbol{y}}) = \underline{\boldsymbol{w}}^t \underline{\boldsymbol{y}} = 0.58y_{\mathrm{HR,HF}} - 0.78y_{\mathrm{TFI,HF}} - 0.24y_{\mathrm{RF,LF}}. \quad (15)$$

If normal distributions are assumed, the minimum error probability decision boundary is -0.77. The adaptation index is then

$$l(\underline{\boldsymbol{y}}) = 0.58y_{\mathrm{HR,HF}} - 0.78y_{\mathrm{TFI,HF}} - 0.24y_{\mathrm{RF,LF}} + 0.77. \quad (16)$$

In Fig. 8(a) we show the result of applying the above index to the same data as in Fig. 6 (taken near the end of pre- and post-SW supine rest periods). Here we see that Fisher's discriminant for the combined feature vector demonstrates increased separation and reduced deviation over any single variable. Therefore, if we treat the discriminant for the combined feature vector as an index of adaptation to weightlessness, a consistent adaptation across all subjects is observed.

It is worth noting that if the two classes, G_0 and G_1, have unequal variance, Fisher's linear discrimination function may

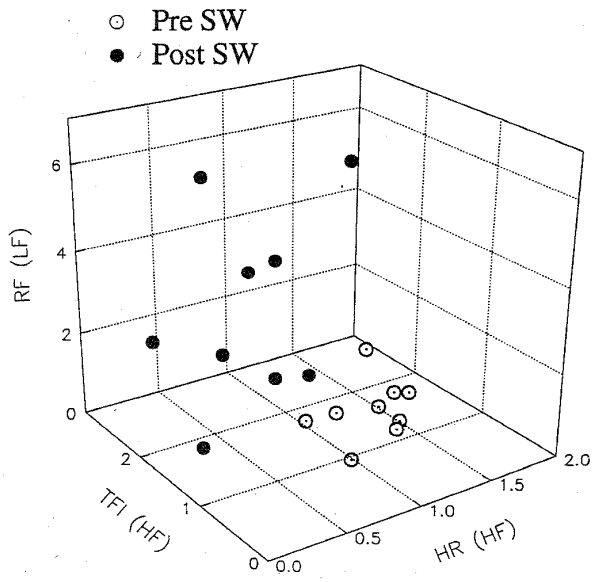

Fig. 7. A sample space spanned by HR (HF), TFI (HF), and RF (LF).

not be optimal. Bayes' quadratic discriminant function [31] may be used (if normal distributions are assumed) such that

$$q(\underline{y}) = \ln \frac{|S_1|}{|S_0|} + (\underline{y} - \underline{m}_1)^t S_1^{-1} (\underline{y} - \underline{m}_1) - (\underline{y} - \underline{m}_0)^t S_0^{-1} (\underline{y} - \underline{m}_0). \quad (17)$$

It is evident that if G_0 and G_1 have identical variance, the quadratic discriminant function is reduced to the linear discriminant function. Therefore, the linear discriminant function performs as well as the quadratic function unless there is a large difference in the covariance matrix. Bayes' quadratic discriminant for the same data set is shown in Fig. 8(b).

Lilliefors' procedure [27] was used to test the validity of the normality assumption. The hypothesis that the two classes are normally distributed could not be rejected at the 0.05 level and therefore a normal distribution of data in these classes may be assumed.

As seen in Fig. 3, CV variable spectra demonstrate large variance across time due to the "noisy" nature of the cardiovascular system. When the index is used to continuously monitor the adaptation, presmoothing is necessary to eliminate occasional, noise-like transient components and thereby increase the immunity to noise and reduce the risk of making a wrong decision based on transient outlier data. Many data smoothing schemes are available. The simplest one is linear smoothing such as Hanning low-pass filtering. The drawback is that linear filtering is sensitive to outlier data, while some types of nonlinear smoothing, such as median filtering, have the advantage of being less sensitive to outlier data. In the present study, a median filter, used to eliminate outliers, followed by a Hanning filter, demonstrated reasonable performance.

Fig. 9 shows the index (and its spectral components) applied to the test subject pre- and post-SW and at intermediate stages of the SW protocol. Adaptation similar to the set of nine subjects (Fig. 8) was observed in this test subject.

V. Discussion

The weightlessness simulation protocol resulted in a negative fluid balance which resulted in significant decreases in stroke volume and central venous pressure. The AP regulatory response of the system, however, compensated for the decrease in fluid volume by increasing resistance mediated by increasing plasma levels of renin and norepinephrine (an independent marker of increased sympathetic activity). The lack of change in the resting HR, in spite of increased sympathetic activity, is not surprising since peripheral vascular resistance increased, thereby compensating for the SV decrease. The combination of negative fluid balance with decreases in mean CVP and SV and increases in plasma renin and norepinephrine are in general agreement with those from other studies of simulated weightlessness [1], [2], [4], [5], indicating increased sympathetic activity in response to decreased plasma volume. Inflight CV data are rare, but at least one study reported that sympathetic indices (norepinephrine, HR) were decreased during flight while the post flight response to standing was characterized by reduced parasympathetic and increased sympathetic activity [32].

With respect to the physiological interpretation of the spectral contents of CV variables, studies in dogs and humans indicate that HF oscillations in HR are mediated by the parasympathetic branch of the autonomic nervous system. It has been shown, in dogs, that LF oscillations in HR are mediated by the sympathetic nervous system [14]. In humans, some investigators [17] have found that LF oscillations were influenced by both the parasympathetic and sympathetic branches of the autonomic nervous system, while others [18], [19] concluded that an increase in the LF power was indicative of increased sympathetic influence on the CV regulatory system. With respect to our model of simulated weightlessness, we previously determined that the spectral contents of CV variables indicated a shift in sympathovagal balance toward enhanced sympathetic influence [22].

In the present study, we interpret our spectral results to indicate a similar shift toward enhanced sympathetic control: 1) the significant decrease in the HF component of HR power after simulated weightlessness indicated a shift toward decreased parasympathetic control of HR [Fig. 5(a)] and 2) the increased LF power in RF [Fig. 5(b)], implicated an increase in sympathetic control of vasomotion. The significant increase in HF power of TFI [Fig. 5(c)] could be due either to an increase in tidal volume or to a change in neural control of respiratory parameters, but the present results offer no evidence to relate this parameter to sympathetic/parasympathetic balance.

Our data also indicated that the level of change due to simulated weightlessness varied from variable to variable and subject to subject. That is, some subjects showed larger changes in some CV variables but less change in other variables (Fig. 6), indicating that the spectral components of a single variable may be limited as a dependable index of cardiovascular adaptation to weightlessness.

To build a robust adaptation index, we formed a feature space spanned by the most important features, HR (HF), TFI (HF), and RF (LF), as determined by the backward elimination algorithm. These features were further linearly combined to

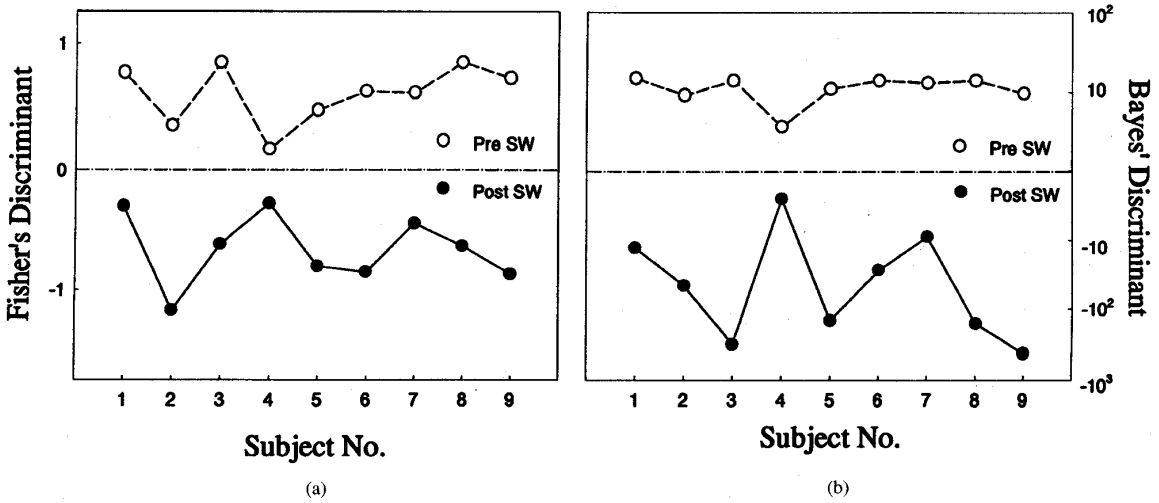

Fig. 8. (a) Fisher's linear discriminant and (b) Bayes' quadratic discriminant for combined features of HR (HF), TFI (HF), and RF (LF) for nine subjects.

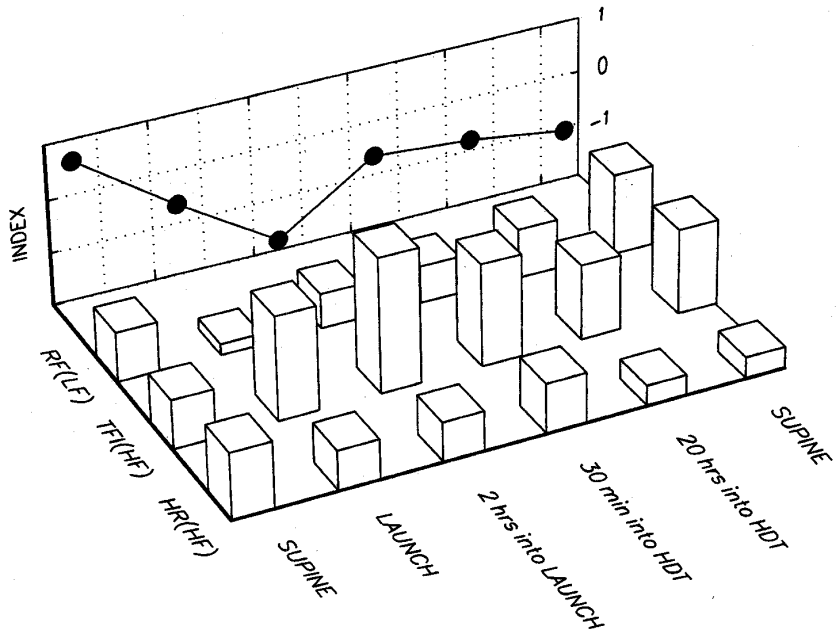

Fig. 9. Adaptation index (Fisher) applied to the test subject pre- and post-SW and all intermediate stages of the SW protocol. The spectral components are also shown.

form an optimal index using Fisher's linear discriminant function which combines features according to the relative importance of discriminant information contained in each feature. Results showed that this integrated and optimized index demonstrated improved discriminatory performance over any single variable. It is worth noting that a multifeature index is not necessarily always better than a single-feature index unless they are appropriately screened and combined in an optimal way.

In conclusion, we verified that the spectral powers in LF and/or HF of some CV variables are promising as a feature space for discrimination of human cardiovascular deconditioning produced by simulated weightlessness. We found that cardiovascular adaptation to simulated weightlessness could be characterized by changes in LF and/or HF spectral power of HR, TFI, and RF. However, due to the large variance across subjects, the reliability of any single variable as an index of cardiovascular adaptation to simulated weightlessness was limited. Discriminatory performance was improved by using multiple CV variables with Fisher's linear discriminant or Bayes' quadratic discriminant function. The ability to discriminate between subjects before and after simulated

weightlessness has the potential for use as an index to track adaptation and prescribe countermeasures to the effects of weightlessness.

ACKNOWLEDGMENT

The authors gratefully acknowledge the staff of the Center for Biomedical Engineering, particularly C. Martin and C. Woolfolk who assisted in the instrumentation set-up and data collection and Dr. M. Berk of the Division of Cardiology who served as medical monitor for this project.

REFERENCES

[1] F. A. Gaffney, J. V. Nixon, E. S. Karlsson, W. Campbell, A. B. Dowdey, and G. C. Blomqvist, "Cardiovascular deconditioning produced by 20 hours of bedrest with head-down tilt (−5°) in middle-aged healthy men," *Am. J. Cardiol.*, vol. 56, pp. 634–638, 1985.

[2] J. V. Nixon, R. G. Murray, C. Bryant, R. L. Johnson, Jr., J. H. Mitchell, O. B. Holland, C. Gomez-Sanchez, P. Vergne-Marini, and C. G. Blomqvist, "Early cardiovascular adaptation to simulated zero gravity," *J. Appl. Physiol.: Respirat. Environ. Exercise Physiol.*, vol. 46, pp. 541–548, 1979.

[3] A. Nicogossian, S. L. Pool, and P. C. Rambaut, "Cardiovascular responses to space flight," *Physiologist*, vol. 26, suppl., pp. 5–78, 1983.

[4] C. M. Lathers, P. H. Diamandis, J. M. Riddle, C. Mukai, K. F. Elton, M. W. Bungo, and J. B. Charles, "Acute and intermediate cardiovascular responses to zero gravity and to fractional gravity levels induced by head-down or head-up tilt," *J. Clin. Pharmacol.*, vol. 30, pp. 494–523, 1990.

[5] ——, "Orthostatic function during a stand test before and after head-up or head-down bedrest," *J. Clin. Pharmacol.*, vol. 31, pp. 893–903, 1991.

[6] J. B. Charles and C. M. Lathers, "Cardiovascular adaptation to space flight," *J. Clin. Parmacol.*, vol. 31, pp. 1010–1023, 1991.

[7] J. B. Charles and M. W. Bungo, "Post-space flight changes in resting cardiovascular parameters are associated with preflight left-ventricular volume," *Aviat. Space Med.*, vol. 57, p. 493, 1986.

[8] F. Baisch, L. Beck, J. M. Karemaker, P. Arbeilles, A. Gaffney, and C. G. Blomqvist, "Head-down tilt bedrest HDT'88—An international collaborative effort in integrated systems physiology," *Acta Physiol. Scand.*, vol. 144, no. S604, pp. 1–12, 1992.

[9] V. A. Convertino, D. F. Doerr, D. L. Eckberg, J. M. Fritsch, and J. Vernikos-Danellis, "Head-down bedrest impairs vagal baroreflex response and provokes orthostatic hypotension," *J. Appl. Physiol.*, vol. 68, pp. 1458–1464, 1990.

[10] J. M. Fritsch, J. B. Charles, B. S. Bennett, M. M. Jones, and D. L. Eckberg, "Short-duration spaceflight impairs human carotid baroreceptor-cardiac reflex responses," *J. Appl. Physiol.*, vol. 73, pp. 664–671, 1992.

[11] H. Lollgen, U. Gebhardt, J. Beier, J. Hordinsky, H. Borger, V. Sarrasch, and K. Klein, "Central hemodynamics during zero gravity simulated by head-down bedrest," *Aerospace Med. Assoc.*, vol. 55, pp. 887–892, 1984.

[12] L. Volicer, R. Jean-Charles, and A. V. Chobanian, "Effects of head-down tilt on fluid and electrolyte balance," *Aviat., Space, and Environ. Med.*, vol. 47, pp. 1065–1068, 1976.

[13] R. W. Gotshall, S. Yumikura, and L. A. Aten, "Effect of the prelaunch position on the cardiovascular response to standing," *Aviat., Space, and Environ. Med.*, vol. 62, pp. 1132–1136, 1991.

[14] A. K. Akselrod, D. Gordon, F. A. Ubel, D. C. Shannon, A. C. Barger, and R. J. Cohen, "Power spectrum analysis of heart rate fluctuations: A quantitative probe of beat-to-beat cardiovascular control," *Sci.*, vol. 213, pp. 220–222, 1981.

[15] J. B. Madwed and R. J. Cohen, "Heart rate response to hemorrhage-induced 0.05-Hz oscillations in arterial pressure in conscious dogs," *Am. J. Physiol.*, vol. 29 (Heart Circ. vol. 4), pp. H1248–H1253, 1991.

[16] J. P. Saul, R. F. Rea, D. L. Eckberg, R. D. Berger, and R. J. Cohen, "Heart rate and muscle sympathetic nerve variability during reflex changes of autonomic activity," *Am. J. Physiol.*, vol. 258 (Heart Circ. Physiol. vol. 27), pp. H713–H721, 1990.

[17] M. Pagani, F. Lombardi, S. Guzzeti, O. Rimoldi, R. Furlan, P. Pizzinelli, G. Sandrone, G. Malfatto, S. Dell'Orto, E. Piccaluga, M. Turiel, G. Baselli, S. Cerutti, and A. Malliani, "Power spectral analysis of heart rate and arterial pressure variabilities as a marker of sympatho-vagal interaction in man and conscious dog," *Circ. Res.*, vol. 59, pp. 178–193, 1986.

[18] M. Pagani, G. Mazzuero, A. Ferrari, D. Liberati, S. Cerutti, D. Vaitl, L. Tavazzi, and A. Malliani, "Sympathovagal interaction during mental stress: A study using spectral analysis of heart rate variability in healthy control subjects and patients with a prior myocardial infarction," *Circ.*, vol. 83, suppl., pp. II43–II51, 1991.

[19] R. D. Berger, J. P. Saul, and R. J. Cohen, "Transfer function analysis of autonomic regulation—I: Canine atrial rate response," *Am. J. Physiol.*, vol. 256 (Heart Circ. Physiol. vol. 25), pp. H142–H152, 1989.

[20] D. Levenhagen, J. Evans, J. Dunworth, M. Berk, and C. Knapp, "Mechanisms of blood pressure maintenance during graded increases of lower body negative pressure (LBNP) before and after 20 hours of 6° head-down bedrest," *FASEB J.*, vol. 4, p. A705, 1990.

[21] D. K. Levenhagen, J. M. Evans, M. Wang, and C. F. Knapp, "Cardiovascular regulation in humans in response to oscillatory lower body negative pressure," *Am. J. Physiol.*, vol. 267 (Heart Circ. Physiol. vol. 36), pp. H593–H604, 1994.

[22] A. R. Patwardhan, D. R. Brown, D. K. Levenhagen, K. J. Grande, J. M. Evans, and C. F. Knapp, "Effect of 22 hours of 6° head-down bedrest on spectral components of resting cardiovascular variables in humans," *FASEB J.*, vol. 5, p. A1038, 1991.

[23] L. S. Goodman and A. G. Gilman, *The Pharmacological Basis of Therapeutics*. New York: Macmillan, 1985.

[24] J. P. Burg, "Maximum entropy spectral analysis," Ph.D. dissertation, Dept. Geophysics, Stanford Univ., Stanford, CA, May 1975.

[25] H. Akaike, "Fitting autoregressive models for prediction," *Ann. Inst. Statist. Math.*, vol. 21, pp. 243–247, 1969.

[26] G. M. Jenkins and D. G. Watts, *Spectral Analysis and Its Applications*. Oakland, CA: Holden–Day, 1968.

[27] J. D. Gibbons and S. Chakraborti, *Nonparametric Statistical Inference*. New York: Marcel Dekker, 1992.

[28] R. Duda and P. Hart, *Pattern Classification and Scene Analysis*. New York, Wiley, 1981.

[29] G. B. Wetherill, P. Duncombe, M. Kenward, J. Kollerstrom, S. R. Paul, and B. J. Vowden, *Regression Analysis with Applications*. New York: Chapman & Hall, 1986.

[30] C. R. Rao, "Inference on discriminant function coefficients," in *Essays in Probability and Statistics*, R. C. Bose, *et al.*, Eds. Chapel Hill, NC: Univ. of North Carolina, 1970, pp. 587–602.

[31] M. James, *Classification Algorithms*. New York: Wileys, 1985.

[32] J. M. Fritsch-Yelle, J. B. Charles, M. M. Jones, L. A. Beightol, and D. L. Eckberg, "Space flight alters autonomic regulation of arterial pressure in humans," *J. Appl. Physiol.*, vol. 77, pp. 1776–1783, 1994.

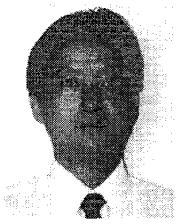

Mao Wang was born in 1962. He received the B.S. degree and M.S. degree in electrical engineering from Nanjing Institute of Technology, Jiangsu, China, in 1984 and 1987, respectively. He received the M.S. degree in biomedical engineering in 1992 and the Ph.D. degree in electrical engineering in 1995 from the University of Kentucky, Lexington.

He is currently a Senior Engineer at Motorola Cellular Infrastructure Group, Arlington Heights, IL. His research interests include signal and image processing, statistical pattern recognition and discrimination, and digital communications.

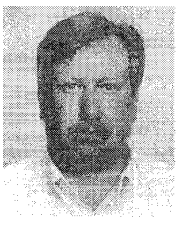

Laurence Hassebrook (M'90) received the B.S.E.E degree from University of Nebraska, Lincoln, in 1979, the M.S.E.E. degree from Syracuse University, Syracuse, NY, in 1987, and the Ph.D. degree in electrical and computer engineering from Carnegie Mellon University, Pittsburgh, PA, in 1990.

He worked at Lincoln Electric System Corp. from 1980–1981. From 1981–1987, he worked at IBM Corporation in Endicott, NY. He is presently an Assistant Professor of Electrical Engineering at the University of Kentucky, Lexington. His interests are in the area of signal processing, structured light illumination, automatic object recognition, and discrimination. Dr. Hassebrook is a member of the Pattern Recognition Society, SPIE, and OSA.

Joyce Evans was born in Mayfield, KY, on December 29, 1937. She received the B.A. and M.S. degrees in physics from Murray State University, Murray, KY, in 1966 and 1968, respectively.

Since 1970, she has worked as a Biomedical Scientist at the Center for Biomedical Engineering, University of Kentucky, Lexington, KY. Her research interests are neural and hormonal components of the cardiovascular system's regulatory response to volume perturbations.

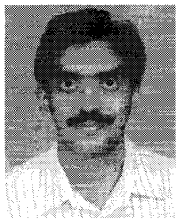

Tomy Varghese (M'95) received the B.E. degree in instrumentation technology from the University of MySore, India, in 1988, and the M.S. and Ph.D. degrees in electrical engineering from the University of Kentucky, Lexington, KY, in 1992 and 1995, respectively.

He is currently a Postdoctoral Research Associate at the University of Texas, Houston. His current research interests include detection and estimation theory, statistical pattern recognition, tissue characterization, and signal/image processing applications in medical imaging.

Dr. Varghese is a member of Eta Kappa Nu.

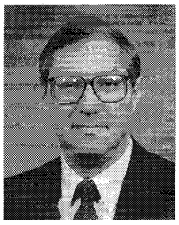

Charles Knapp (A'90) was born in Evansville, IN on March 28, 1940. He received the B.A. degree from St. Procopius College, Lisle, IL, in 1962 and the B.S., M.S., and Ph.D. degrees in aerospace engineering from Notre Dame University, Notre Dame, IN, in 1963, 1965, and 1968, respectively.

He joined the faculty of the Department of Mechanical Engineering at the University of Kentucky, Lexington, in 1968 where he conducted biomedical engineering research in the Wenner–Gren Laboratory. He is presently Professor and Director of the University of Kentucky's Center for Biomedical Engineering. His current research interest is in understanding mechanisms associated with changes in autonomic regulation of cardiovascular function during hypo/hypergravity challenges.